Numerical Study of Fluxon Solutions of Sine-Gordon Equation under the Influence of the Boundary Conditions

Pavlina Khristova Atanasova[1], Elena Valerievna Zemlyanaya[2], and Yury Shukrinov[2]

[1] Plovdiv University "Paisii Hilendarski", 4000 Plovdiv, Bulgaria
[2] Joint Institute for Nuclear Research, 141980 Dubna, Russia
{poli,elena}@jinr.ru, shukrinv@theor.jinr.ru

Abstract. The dependence on the boundary conditions of the fluxon solutions of a boundary problem for the sine-Gordon equation (SGE) is investigated numerically. Interconnection between fluxon and constant solutions is analyzed. Numerical results are discussed in the context of the long Josephson junction model.

Keywords: long Josephson junction, sine-Gordon equation, Sturm-Liouville problem, Newton's method, fluxon, bifurcation, numerical continuation.

1 Introduction

The sine-Gordon equation is a nonlinear hyperbolic partial differential equation involving the d'Alembert operator and the sine of the unknown function. The equation reads

$$u_{tt} - u_{xx} + \sin u = 0 \ , \tag{1}$$

where $u = u(x,t)$. It arises in differential geometry and various areas of physics, including applications in relativistic field theory, Josephson junctions (JJs) or mechanical transmission lines. The stack of coupled JJs describing by system of coupled sine-Gorgon equations is actively investigated [6,7,8].

In the framework of the long JJs model, the dynamics of the magnetic flux in a JJ of length $2l$ is described by the perturbed sine-Gordon equation:

$$\varphi_{xx} - \varphi_{tt} - \alpha\varphi_t = \sin\varphi - \gamma \, , \quad t > 0 \, , \quad x \in (-l, l) \tag{2}$$

with boundary conditions

$$\varphi_x(\pm l, t) = h_e \ , \tag{3}$$

where φ is the magnetic flux distribution, h_e – the external magnetic field, γ – the external current and $\alpha \geq 0$ – the dissipation coefficient.

The aim of this work is a numerical investigation of the properties of the *static* fluxon solutions of Eq. (2) under the influence of the external magnetic field parameter h_e in (3). Such solutions satisfy the following boundary problem

G. Adam, J. Buša, and M. Hnatič (Eds.): MMCP 2011, LNCS 7125, pp. 201–206, 2012.

$$-\varphi_{xx} + \sin\varphi - \gamma = 0\,, \quad x \in (-l; l)\,, \quad \varphi_x(\pm l) = h_e\ . \tag{4}$$

Here, we only consider the case of the JJ length $2l = 10$ with zero external current $\gamma = 0$.

2 Numerical Approach

The static fluxon solutions of Eq. (2) are obtained numerically by solving the boundary problem (4). The stability analysis is based on the numerical solution of the following Sturm-Liouville problem [5]

$$-\psi_{xx} + q(x)\psi = \lambda\psi\,, \quad \psi_x(\pm l) = 0\,, \quad q(x) = \cos\varphi(x,p)\,, \quad p = (l, h_e, \gamma)\,. \tag{5}$$

In this approach, the minimal eigenvalue of Eq. (5) $\lambda_0(p) > 0$ corresponds to a stable solution. If $\lambda_0(p) < 0$, the solution $\varphi(x,p)$ is unstable. The case $\lambda_0(p) = 0$ indicates a bifurcation with respect to one of parameters $p = (l, h_e, \gamma)$.

The numerical solution of Eq. (4) is based of the continuous analog of Newton's method [9]. At each Newtonian iteration the corresponding linearized problem is solved on a uniform grids with 1025 number of nodes, using a three-point Numerov approximation of the fourth order accuracy [11].

For numerical solution of the Sturm-Liouville problem (5) we applied the standard three-point second order finite-difference formulae. First several eigenvalues of the resulting algebraic three-diagonal eigenvalue problem are obtained by means of the standard EISPACK code. Details of the numerical scheme are described in [1,2,4] for the double sine-Gordon equation.

The known at $h_e = 0$ solutions M_0 and Φ^1 are numerically path-followed to non-zero positive h_e. At each ith step of the numerical continuation we analyze the stability of the solution $\varphi(x, h_e^{(i)})$ and calculate the following physical characteristics:

- full magnetic flux of the distribution $\Delta\varphi^{(i)} = \varphi(l, h_e^{(i)}) - \varphi(-l, h_e^{(i)})$;
- quantity N denoted "number of fluxons" in [4] is determined as follows

$$N[\varphi(x, h_e^{(i)})] = \frac{1}{2l\pi}\int\limits_{-l}^{l} \varphi(x, h_e^{(i)})\, dx\ . \tag{6}$$

Since each solution φ of Eq. (4) is defined with an accuracy $2k\pi$ ($k \in \mathbf{Z}$) then the value $N[\varphi]$ is defined with accuracy $2k$. The arbitrariness at the choice of integer number k can be used for the "concordance" of the value N with the value of the full magnetic flux $\Delta\varphi$ according to the condition

$$|N[\varphi] - \Delta\varphi/2\pi| \to \min\ . \tag{7}$$

Below, similar to [1,2,3,4], the solutions φ with $n = N$, where N satisfies Eq. (7), are denoted φ^n.

The crossing through the turning points in the numerical continuation (where the moving direction along the curve $\Delta\varphi(h_e)$ changes as we follow on the new branch) was organized as in [10]. The turning points are identified with the help of the relation that is tested at each ith step of numerical continuation:

$$\left| \frac{{h_e}^{(i)} - {h_e}^{(i-1)}}{\Delta\varphi^{(i)} - \Delta\varphi^{(i-1)}} \right| < \varepsilon \ , \tag{8}$$

where $\varepsilon > 0$ is a small known quantity. Note that (8) is a simple approximation of the equality $dh_e/d\Delta\varphi = 0$ which is valid at the turning points of the curve $\Delta\varphi(h_e)$. In case we run into a turning point the sign of the h_e-increment is to be changed. At each step of the numerical continuation, the initial guess for Newtonian process was chosen of the form

$$\varphi(h_e^{(i+1)}) = \varphi(h_e^{(i)}) + (h_e^{(i+1)} - h_e^{(i)}) \cdot \frac{\varphi(h_e^{(i)}) - \varphi(h_e^{(i-1)})}{h_e^{(i)} - h_e^{(i-1)}} \tag{9}$$

which prevents the continuation from reversing to the previous branch of $\Delta\varphi(h_e)$.

3 Numerical Results

Two *basic* distributions are known at $h_e = 0$: the uniform Meissner solution M_0 with $N[M_0] = 0$ and the fluxon solution Φ^1 with $N[\Phi^1] = 1$ ([4]). The lowest eigenvalue λ_0 of Eq. (5) is negative for Φ^1 and positive for M_0. Under increasing $h_e > 0$, the eigenvalue λ_0 of the basic state M_0 stays positive, i.e., the branch is stable until $h_e = 2$. In the Φ^1 case, the lowest eigenvalue λ_0 crosses zero at the point $h_e = h_1 = 0.054$, i.e., the branch is unstable for $0 \le h_e \le h_1$ and stable for $h_1 < h_e < 2.098$. The transformation of the internal magnetic field shape of the basic solutions in terms of h_e is shown in Figs. 1, 2.

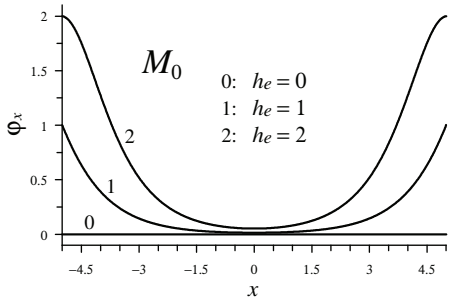

Fig. 1. Internal magnetic field distribution $\varphi_x(x)$ associated with the state M_0 for several values of the magnetic field h_e

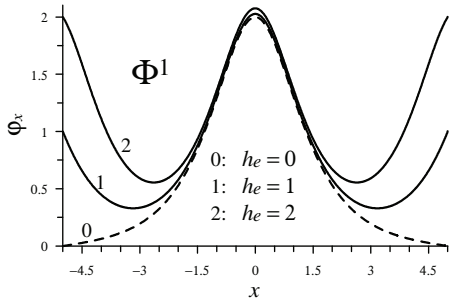

Fig. 2. Internal magnetic field distribution $\varphi_x(x)$ associated with the state Φ^1 for several values of magnetic field h_e

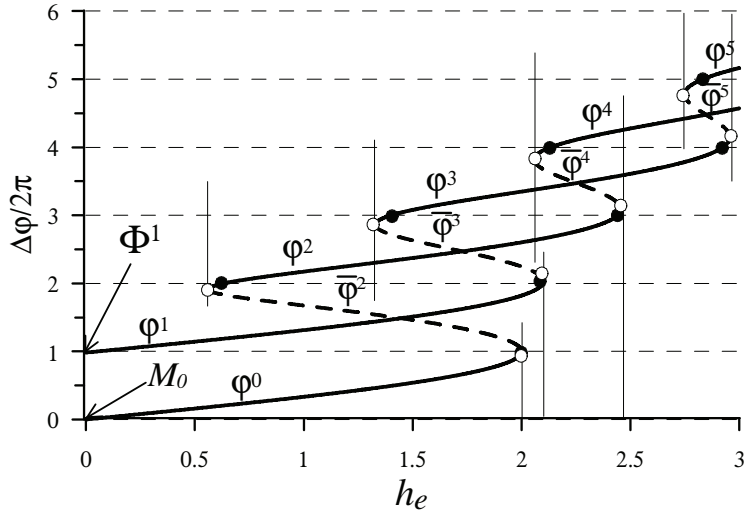

Fig. 3. Dependence of the full magnetic flux $\Delta\varphi$ on the magnetic field h_e for fluxon distributions associated with M_0 and Φ^1. Solid and dashed lines correspond, respectively, to the stable and unstable states. Light circles indicate the turning points, dark circles indicate the points, where the solution stability changes.

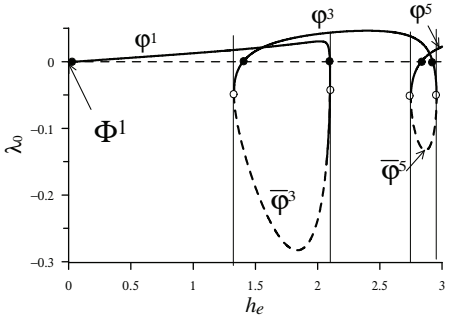

Fig. 4. Dependence of the lowest eigenvalue λ_0 on the magnetic field h_e for the branch associated with Φ^1. Light circles indicate the turning points, dark circles indicate the points of stability change.

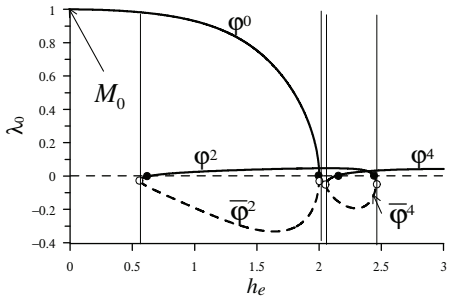

Fig. 5. Dependence of the lowest eigenvalue λ_0 on the magnetic field h_e for the branch associated with M_0. Light circles indicate the turning points, dark circles indicate the points of stability change.

The $\Delta\varphi(h_e)$ dependences of the branches associated with the basic solutions M_0 and Φ^1 are plotted in Fig. 3. The data show that at some points (light circles in Fig. 3) the curves $\Delta\varphi(h_e)$ turn back to another, upper, branches. When the $\Delta\varphi(h_e)$ curve turns to the left ("$\supset$"-point) the quantity N is increased to $N+2$. Therefore, the branch stemming from the basic M_0 solution at $h_e = 0$ joins the

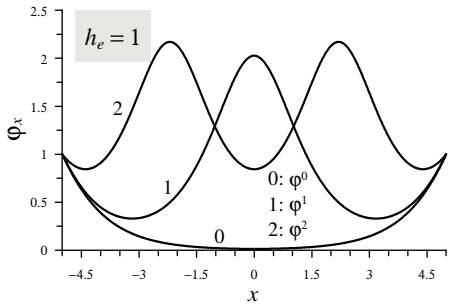

Fig. 6. Coexisting stable internal magnetic field distributions φ_x at magnetic field $h_e = 1$

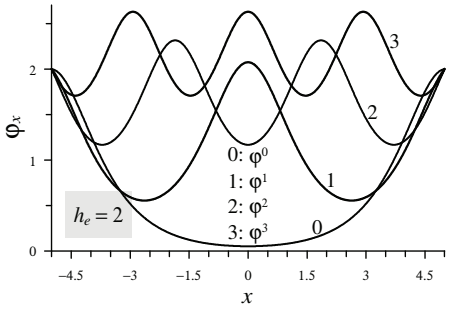

Fig. 7. Coexisting stable internal magnetic field distributions φ_x at magnetic field $h_e = 2$

fluxons (stable and unstable) with the even N, while the other branch (associated with the Φ^1 basic fluxon) connects fluxons (stable and unstable) with the odd N.

The change of stability occurs at the points (marked by dark circles in Fig. 3) where the $\lambda_0(h_e)$ curve crosses zero, see Figs. 4, 5. The "$\supset$"- and "$\subset$"-turning points are indicated by the light circles. The "$\subset$"-turning points connect a pair of unstable solutions with the same number N: φ^n and $\bar{\varphi}^n$. An increase of N to $N + 2$ is observed at the "$\supset$"-turning points (light circles).

Thus, for $0 < h_e < h_1$ we have a single stable static distribution (associated with the basic solution M_0). For $h_1 < h_e < h_{cr}$, $h_{cr} = 0.561$ this distribution coexists with another one associated with the basic solution Φ^1. The increase of the magnetic field h_e leads to the appearence, at h_{cr}, (most left light circle in Fig. 3) of a pair of (unstable) states (φ^2, $\bar{\varphi}^2$). As h_e is growing further, the stabilization of $\bar{\varphi}^2$ occurs (most left dark circle in Fig. 3), i.e. for $h_e = 1$ there are three stable distributions coexisting with the unstable state φ^2, see Fig. 6. Further increase of h_e induces a creation, at each "$\subset$"-point, of an additional pair (φ^n, $\bar{\varphi}^n$) with growing n, see Fig. 7. At the same time, the pairs ($\varphi^n, \bar{\varphi}^{n+2}$) with previous values n are sequentially disappearing at the "$\supset$"-points.

4 Conclusions

The detailed information on the variation of the fluxon structure with the external magnetic field in a long Josephson junction is very important for the correct interpretation of the experimental results. In this paper we investigated the dependence of the stationary fluxon solutions of Eq. (2)–(3) in terms of the external magnetic field h_e. Our numerical technique allowed us to establish the interconnection between the basic solution M_0 at $h_e = 0$ and the stationary distributions φ^n with even numbers n as well as the interconnection between the basic state Φ^1 at $h_e = 0$ and φ^n with odd numbers n. Coexistence of different stable n-fluxon distributions at different values of the external magnetic field

h_e has been established. We consider that the predicted transformations of the stable fluxon distributions can be observed experimentally by investigation of the critical current in terms of the external magnetic field.

Acknowledgments. The work was supported by the Program for collaboration of JINR (Dubna) and Bulgarian scientific centers. EVZ was partially supported by RFBR (Grant No. 09-01-00770). PKhA was partially supported by project NI11-FMI-004.

References

1. Atanasova, P.K., Boyadjiev, T.L., Zemlyanaya, E.V., Shukrinov, Y.M.: Numerical Study of Magnetic Flux in the LJJ Model with Double Sine-Gordon Equation. In: Dimov, I., Dimova, S., Kolkovska, N. (eds.) NMA 2010. LNCS, vol. 6046, pp. 347–352. Springer, Heidelberg (2011)
2. Atanasova, P.K., Boyadjiev, T.L., Shukrinov, Y.M., Zemlyanaya, E.V.: Numerical investigation of the second harmonic effects in the LJJ (2010) arXiv:1005.5691v1
3. Atanasova, P.K., Boyadjiev, T.L., Shukrinov, Y.M., Zemlyanaya, E.V., Seidel, P.: Influence of Josephson current second harmonic on stability of magnetic flux in long junctions. J. Phys. Conf. Ser. 248, 012044 (2010) arXiv:1007.4778v1
4. Atanasova, P.K., Zemlyanaya, E.V., Boyadjiev, T.L., Shukrinov, Y.M.: Numerical modeling of long Josephson junctions in the frame of double sine-Gordon equation. Mathematical Models and Computer Simulations 3(3), 388–397 (2011)
5. Galpern, Y.S., Filippov, A.T.: Joint solution states in inhomogeneous Josephson junctions. Sov. Phys. JETP 59, 894 (1984) (Russian)
6. Hu, X., Lin, S.Z.: Phase dynamics in a stack of inductively coupled intrinsic Josephson junctions and terahertz electromagnetic radiation. Supercond. Sci. Technol. 23, 053001 (2010)
7. Koshelev, A.E.: Stability of dynamic coherent states in intrinsic Josephson-junction stacks near internal cavity resonance. Phys. Rev. B. 82, 174512 (2010)
8. Krasnov, V.M.: THz emission from intrinsic Josephson junctions at zero magnetic field via breather auto-oscillations. Phys. Rev. B. 83, 174517 (2011)
9. Puzynin, I.V., Boyadzhiev, T.L., Vinitskii, S.I., Zemlyanaya, E.V., Puzynina, T.P., Chuluunbaatar, O.: Methods of Computational Physics for Investigation of Models of Complex Physical Systems. Physics of Particles and Nuclei 38(1), 70–116 (2007)
10. Zemlyanaya, E.V., Barashenkov, I.V.: Numerical study of the multisoliton complexes in the damped-driven NLS. Math. Modelling 16(3), 3–14 (2004) (Russian)
11. Zemlyanaya, E.V., Puzynin, I.V., Puzynina, T.P.: PROGS2H4 – the software package for solving the boundary probem for the system of differential equations. JINR Comm. P11-97-414, Dubna, 18 (1997) (Russian)